LIKELIHOOD AND CONSEQUENCES OF FUEL STRING COMPRESSION AT POINT LEPREAU GENERATING STATION

P.J. REID

ALARA Research, Inc., 975 First Avenue, Saint John, NB, E2M 4N9

R.A. GIBB

New Brunswick Power, Point Lepreau Generating Station, P.O. Box 10, Lepreau, NB, E0G 2H0

During an accident which results in fuel heatup, axial thermal expansion of the fuel string relative to the pressure tube will occur. If the temperature transient is sufficiently severe, the fuel string may contact the shield plugs at both ends of the channel. Any additional axial thermal expansion will result in deformation of fuel and fuel channel components, leading to tensile or compressive stresses in the different fuel channel components. If these loads become sufficiently large, they could result in failure of a fuel channel component or to channel failure due to bending of a fuel element under load. The analysis described in this paper demonstrates that this process would not result in fuel channel failure for a design basis accident at Point Lepreau Generating Station (PLGS), even if the station were retubed to "as-built" channel lengths.

INTRODUCTION

In the following paragraphs, a brief description of the physical behaviour of the fuel and fuel channel components under load will be presented. This behaviour was modelled for this analysis using the computer program COMPRESS, version 1.0 (Reference (1)).

At the very beginning of the transient, before contact between the fuel string and the ends of the fuel channel, the fuel elements will expand. Any remaining axial clearance between the fuel pellet stack and the endcaps will be consumed. Then the pellet stack will stretch the fuel sheath, causing minor deformation of the endcap due to the load required to deform the sheath. This will occur because the thermal expansion coefficient of Zircaloy is smaller than that of UO_2.

Once the fuel string contacts the ends of the fuel channel, any further expansion is accommodated by deformation, which will be accompanied by axial loads. The magnitude of these loads depends on the elastic/plastic deformation behaviour of fuel and channel components. All of the fuel channel components which experience load will deform to some extent, both elastically and plastically. Some of the more important deformation processes are as follows.

The dominant source of deformation modelled for this analysis is plastic creep of the endcaps and endplates of the bundles, *i.e.* the bundle junctions. This is because the bundle junctions are heated to relatively high temperatures during the fuel channel heatup due to their thermal proximity to the fuel pellet stack. Above 800°C, the Zircaloy of the endcaps will convert to β-phase, which has very little strength and deforms easily under load due to creep. This sort of deformation is strain *rate* dependent (*i.e.* $F \propto \dot{\varepsilon}$). This is different than normal elastic deformation, which is strain dependent (*i.e.* $F \propto \varepsilon$). This fact has important consequences regarding the definition of the limiting accident scenario, since it implies that an accident with a given amount of required compression over a short time interval is more limiting than an accident with the same amount of required compression over a long time.

While deformation of the bundle junctions is the most important contributor to the deformation, there are other significant processes as well. For example, the fuel elements themselves will deform elastically and plastically, and the normally present cracks in the irradiated fuel will close under the load. Also, the pressure tube material, while significantly cooler than the bundle junctions, will deform elastically, due to its relatively small cross-sectional area. All of the other fuel channel components which are under load, such as the shield plugs, the shield plug jaws and the end fittings, will also deform. These deformations will be much smaller than those discussed above, because of their low temperature and the strength of the materials involved.

This paper presents arguments which will show that, if fuel string compression were predicted to occur in a Large Break LOCA at Point Lepreau Generating Station, the resulting loads will bound those which might occur for other design basis accidents. In order to assess what these loads might be, several Large Break LOCA scenarios are examined using the computer codes FACTAR_SS 1.1 (Reference (2)), FACTAR 1.1 (Reference (3)) and COMPRESS 1.0 (Reference (1)). The resulting load predictions are compared to the limiting failure loads to determine whether fuel channel integrity is threatened during the analysed events.

ANALYSIS METHODS AND RATIONALE

In performing this analysis, the intent was to examine the most limiting design basis accident for which data were available. This provides reasonable assurance that this preliminary assessment captures a near-worst-case scenario. The assessment is intended to cover off all design basis accidents even if the station were to be retubed. The smallest gap which still results in no adverse pressure tube integrity concerns is identified, giving an estimate of what the minimum axial gap should be in the event that PLGS is retubed and quantifying the safety margins available in the gaps as they exist at 3880 effective full power days (FPD). The steps of the analysis can be summarised as follows:

1. Determine critical accident. In this step, the accident which would result in the most severe threat to fuel channel integrity is identified. The selection is made from the group of all design basis accidents for which maintenance of fuel channel integrity is required.
2. Determine axial clearance available. Here, the magnitude of the expected axial clearance is determined for both the initial, "as-built" dimensions and the dimensions including creep up until 3880 FPD.
3. Determine the maximum acceptable axial load. Once this is done, the analysis can determine the smallest axial clearance for which the acceptable peak load is not exceeded.
4. Select channels for analysis and perform reactor physics, circuit thermal hydraulics and slave channel analysis. This provides the boundary conditions needed to perform the FACTAR analysis.
5. Perform FACTAR_SS and FACTAR analysis. Here the actual thermal response of the fuel and fuel channel is predicted to determine whether fuel string compression will occur. Sensitivity studies are performed to address uncertainties in initial conditions.
6. Determine the smallest axial clearance for which the maximum acceptable load is not exceeded. A series of COMPRESS runs must be performed here. Once this is done, the implications of the minimum axial clearance for future reactor operations can be assessed.

Determining Critical Accident Scenario

As discussed in the Introduction, some of the most important strain processes are plastic deformation of the Zircaloy in the bundle endcaps and endplates, elastic deformation of the pressure tube and elastic deformation of the fuel elements. The strain deformation of endcaps and endplates, because of their small cross-sectional areas and relative weakness (they are likely to be ≥ 800°C at the time of contact due to their proximity to the fuel) will be the most significant. Since plastic deformation of Zircaloy is a rate-dependent process, this implies that the accident which results in the highest rate of increase in fuel temperature (and hence in the highest strain rates) will be the one which results in the greatest axial load transient, as long as the heatup is sufficient to result in contact with the ends of the channel (*i.e.* a scenario with 20 mm strain over 1000 s has lower loads than one with 2 mm of strain in 1 s).

The design basis accident which results in the greatest amount of fuel heatup relative to the pressure tube is a flow blockage event. However, this accident is terminated by pressure tube failure, so it is not necessary to assess whether fuel string compression will result in an earlier channel failure.

The next most severe design basis accident from the perspective of fuel heatup is a LOCA with coincident loss of ECC (LOECC). However, the *rate* of fuel heatup in such scenarios is slow, since the fuel is at decay power levels. Also, in an LOECC the temperature profiles within the fuel are very flat. This implies that the bundle junctions will be quite close to the fuel temperature and, since Zircaloy strain rates have an exponential dependence on temperature, the endcaps will yield under compression. These two factors (low required strain rates and hot bundle junctions) will result in relatively low loads in any LOECC scenario in which fuel string compression occurs. Finally, as the bundles slump, their structural strength becomes negligible and deformation will be possible at very low loads.

The design basis accident which results in the next most severe amount of fuel heatup is a Large Break LOCA. This accident also results in very fast fuel heatup, due to the large positive reactivity insertion caused by the voiding of the coolant through the break. Also, due to the relatively high power levels existing in the first few seconds of the accident, there are large temperature gradients within the fuel elements, meaning that the bundle junctions are significantly cooler than the fuel. Hence this accident category should result in more severe axial loads than an LOECC, if it is found that fuel string compression occurs for a given LOCA case.

Accidents which result in less severe fuel heatup (*i.e.* Small Break LOCA or Loss of Class IV Power) result in less rapid heatup than Large Break LOCA. Also, it is very unlikely that these accidents would result in any axial contact at all since, as will be seen, only the most severe Large Break LOCA cases could result in contact, even for a retubed reactor, and these other scenarios generally result in less severe heatup than Large Break LOCAs. Based on these considerations, the Large Break LOCA scenario was selected for assessment in this study.

The temperature of the fuel land (which is near the fuel surface) is the temperature which is used to determine the axial thermal expansion in the calculation of axial loads. Therefore, the specific Large Break LOCA case selected is that which resulted in the highest fuel sheath temperatures as predicted by FIREBIRD from the most recent assessment of Large Break LOCAs available. This assessment considers the consequences of a 20% RIH, 100% ROH and a 100% PSH break, all of which are critical breaks. The case which resulted in the most severe sheath temperatures (and hence the highest fuel land temperatures) in this assessment was the 100% PSH break.

Assessment of Available Axial Clearance

Minimum axial gaps for both the "as-built" and crept conditions have been calculated for all 380 PLGS fuel channels at normal operating temperatures. The following briefly summarises the results.

Minimum axial gaps were derived from a combination of both design and measured data. To determine the "as-built" minimum axial gap for each fuel channel under normal operating temperatures, the dimensional change associated with thermal expansion for both fuel channel components and fuel bundles was assessed. Table 1 shows the minimum axial gaps for each fuel channel at normal operating temperatures for the "as-built" condition. To assess the impact of pressure tube creep, measured creep rates for each fuel channel were prorated to effective full power day 3880 (May 1994) to determine the net increase in length of each pressure tube. Table 2 shows the minimum axial gap for the crept condition at normal operating temperatures.

The axial gaps in the channels at PLGS with pressure tube creep up to May 1994 are such that, in even the most limiting channel, contact would only occur for an LOECC or a flow blockage event. With a minimum value of ~70 mm for the smallest initial gap, a UO_2 thermal expansion coefficient of ~12 μm/m·K and a fuel string initial length of ~6 m, the channel average fuel land temperature could increase by ~950°C before axial contact would occur. A temperature increase of that magnitude is only found in those two scenarios.

For the "as-built" minimum gaps, fuel string compression could occur for other scenarios, such as a LOCA. The axial gap is treated parametrically in this analysis to determine the smallest acceptable axial gap. The peak load in the case of a LOCA with this initial gap will bound that which would be found for any other scenario at that gap size, as explained above, as long as contact is indeed predicted. This peak load will also, obviously, bound the peak load for any scenario with a larger initial axial gap, such as those obtaining for pressure tube creep up to May 1994.

Acceptable Peak Loads in the Event of Axial Contact

The criterion for acceptability of a predicted axial load is fuel channel component survival. The most limiting components from this point of view are the fuel elements, which may bend into contact with the pressure tube with sufficient normal force to cause a local hot spot, the shield plug jaws, which may shear under load, and the pressure tube rolled joint, which may be pulled out under sufficient load.

In order to determine the buckling load of the fuel element, the Young's modulus of both the fuel and the sheath must be used and the classical Euler's equation solved for the resulting buckling load.

Based upon data by Williford (Reference (4)), a minimum value of the Young's modulus may be determined. Using an initial diametral gap of 0.051 mm in Williford's model, an effective Young's modulus in the range of 30 to 60 GPa is found, depending on the initial power assumed. In this analysis, a Young's modulus of 25 GPa is used for the fuel buckling calculations.

The fuel sheath Young's modulus used is the Young's modulus at 1100°C. Using these two moduli for fuel and sheath material, a fuel element will buckle at 1.6 kN, implying that the outer ring could withstand a peak axial load of 28.8 kN before a fuel element might bend into contact with the pressure tube.

In reality the elements would tend to bend away from the pressure tube. There will be a temperature gradient across the outer elements due to the proximity of the cool pressure tube on their outside. This would result in a thermally-induced stress gradient in the elements, which would cause them to tend to bend towards the centre of the fuel bundle, away from the pressure tube. However, in the case that the fuel elements *do* bend towards the pressure tube, a pressure tube integrity assessment would be required to establish whether fuel channel integrity is maintained. Using fuel element buckling as a measure of acceptability of a given axial gap is done strictly to limit the scope of the analysis undertaken.

Both the shield plug jaws and the pressure tube rolled joint should have temperature transients which do not vary significantly from the normal operating temperature in a LOCA, due to the significant heat capacity and resultant thermal lag of the metal components making up the shield plug/end fitting/pressure tube assembly, which are all in good thermal contact with each other. With the significant fuel string heatup over within the first 25 seconds for a LOCA, these components will not change in temperature to any great degree. Therefore, the strengths of the shield plug jaws and the pressure tube rolled joint should not vary significantly from those under nominal conditions.

The shield plug jaws are constructed of ASTM A 564 Stainless Steel, Type/Grade 630, heat treated at 1025°F. According to Reference (5), this steel has a minimum yield strength of 1000 MPa. Based on the geometry of the shield plug jaws and using the shear strength as being half of the yield strength, the shield plug jaws could withstand a peak load of 315 kN before failure.

The pull-out strength of the pressure tube rolled joint has been determined by testing to be in the range between 614-735 kN.

Based on the above, the most limiting fuel channel component for peak load are the fuel elements themselves, which could bend into contact with the pressure tube at an axial load of as low as 28.8 kN. The other two components have failure loads at least an order of magnitude higher than this. Therefore, in this analysis, the goal is to determine the minimum axial gap at which the peak axial load is predicted to remain less than 28.8 kN.

Reactor Physics and System Thermal Hydraulic Calculations

The most recent assessment of Large Break LOCAs available was used for this analysis. This assessment considered the case of a Large Break LOCA occurring immediately following a return to full power from a long shutdown. The 100% PSH break case was for the nominal flux shape but with high moderator poison concentration to make up for the decay of saturating fission products. The assessment assumed a void reactivity uncertainty of 2.3 mk, and included the effect of pressure tube creep on core voiding.

Slave Channel Calculations - Hydraulic Boundary Conditions

In order to provide a more detailed and accurate assessment of the thermal hydraulic boundary conditions than are possible with a full system simulation, slave channel analysis was performed. Three channels were selected to be studied. These were B10, L11 and O06. These channels are all located in the critical pass of the broken loop. B10 is a high elevation, low power channel; L11 and O06 are mid-elevation, high power channels which are, respectively, inside and outside of the adjuster region. The initial axial power profile in the channels are shown, along with those used in FACTAR sensitivity studies, in Table 4. The axial power profiles used in the FIREBIRD analyses for these channels, which are referred to as "FIREBIRD initial powers" in this paper, were chosen to be consistent with the reactor physics calculations for the system simulation.

The data used to derive the FACTAR input files from these runs are the mid-channel pressure transient, the relative power transient and initial power distribution, the mid-channel flow transient and the enthalpy transients for the middle of the channel and both end fittings.

Bundle Power and Burnup Data for FACTAR_SS Analysis

The first step in determining the fuel and fuel channel thermal/mechanical response is to perform the FACTAR_SS analysis. The results of this analysis provide the initial conditions of the fuel to the subsequent FACTAR analysis. The FACTAR analysis provides fuel and pressure tube transients, as well as other boundary conditions, to the COMPRESS code, which is used to determine the axial thermal expansion of the fuel relative to the pressure tube and the resulting load transient, if any.

FACTAR_SS version 1.1 (Reference (2)) was used to determine the initial condition of the fuel for the FACTAR analysis. FACTAR_SS is a computer code based on ELESIM2.MOD10, and it is used to predict the steady state fuel behaviour of the fuel elements in a single channel.

FACTAR_SS 1.1 was independently developed and tested by Ontario Hydro for use in the analysis of Large Break LOCAs and has undergone verification testing by the developing organisation. In order to ensure that the executable used in this analysis corresponds to the code which is reported in the code documentation, sample cases which were used and referred to in the code document were re-run with the executable used in this analysis. The results of these cases were compared with the results which were created for the code documentation. This comparison showed that the results were identical.

Input parameters used in the FACTAR_SS analysis are listed in Table 3, along with input parameters used in FACTAR and COMPRESS.

The FACTAR_SS analysis requires element descriptive data and power/burnup histories. The element descriptive data are based on the nominal design values. The power/burnup histories are derived from the initial axial and radial power profiles (Table 4 and Table 5), the channel average exit burnup, and the licensing overpower envelope (Figure 1). The selection of power/burnup histories was done in a manner that would allow extension of the analysis to cover a range of powers and burnup consistent with plant operation. A description of this derivation follows.

The power/burnup histories for the FACTAR_SS input files are created by taking the specified axial and radial power profiles, the bundle shift scheme used in fuelling and the average exit burnup which the channel is being fuelled to. The average exit burnup implies a certain dwell between refuellings of the channel. The power/burnup histories of each bundle is such that the channel is either: a) at the end of its dwell (just about to be refuelled), or b) as far through the dwell as is possible without any bundle exceeding the licensing power/burnup envelope. The shape of the power/burnup history is obtained by pro-rating the overpower envelope.

Sensitivity analyses were carried out to determine the effect of variations in channel powers and axial power profiles on the predicted axial loads. In these cases, the three channels were also examined at the maximum possible channel power and the most peaked possible axial power profile. These power profiles are shown in Table 4. The case which resulted in the most severe peak loads of these six cases was used as the basis for all other sensitivity studies, and will be referred to as the reference case in the rest of this section.

Additional sensitivity studies were also carried out for the reference case. These studies were designed to assess the impact of the average exit burnup assumed in deriving the power/burnup histories of the channels. The fuel to sheath heat transfer coefficient is dependent on the power/burnup history. Higher burnups mean lower fuel to sheath heat transfer coefficients and hence higher peak temperatures in a LOCA transient. However, a sufficiently high burnup results in a reduction in power. The effect of the power/burnup history on temperatures and on axial thermal expansion and peak axial load must therefore be investigated. To do this, the reference case is used for a sensitivity study in which the average exit burnup is varied from 10 MW·h/kgU and 340 MW·h/kgU. For those cases in which the average exit burnup is high (*i.e.* 200 MW·h/kgU and above), it was necessary to reduce the assumed channel power in order to allow the channel to reach the specified average exit burnup without exceeding the power/burnup envelope.

FACTAR Analysis

FACTAR version 1.1 (Reference (3)) was used to determine the fuel and channel transient thermal response during the transient. FACTAR 1.1 is a computer code developed to simulate the transient thermal and mechanical behaviour of the fuel bundles within a single CANDU fuel channel for a range of accident conditions including small and large break LOCAs. It consists of a flow-ring thermal hydraulics model, coupled with a detailed mechanistic fuel model which is based upon a slightly modified version of ELOCA.mk4.

FACTAR 1.1 was independently developed and tested by Ontario Hydro for use in the analysis of Large Break LOCAs and has undergone verification testing by the developing organisation. In order to ensure that the executable used in this analysis corresponds to the code which is reported in the code documentation, sample cases which were used and referred to in the code document were re-run with the executables used in this analysis. The results of these cases were compared with the results which were created for the code documentation. This comparison showed that the results were identical.

The FACTAR analysis uses the initial conditions predicted by the FACTAR_SS analysis along with prescribed transient boundary conditions to predict fuel and fuel channel temperature transients for the postulated Large Break LOCA case. The various input parameters required by the FACTAR input file are shown in Table 3, along with those input parameters used in the FACTAR_SS and COMPRESS analyses.

Most of the input parameters are derived from the Fuel Design Manual, from design drawings or from consideration of the important physical processes in Large Break LOCAs. The exceptions are the fuel element stack length and the transient boundary conditions of channel pressure, incoming coolant enthalpy, channel flow and the power transient.

The fuel stack length used in the FACTAR runs was chosen to be consistent with that assumed in the COMPRESS code. COMPRESS assumes that the bundle is at the maximum possible length as per the manufacturer's drawings with an additional strain of 0.4% which corresponds to observed strain under normal operating conditions (NOC).

The transient boundary conditions used in the FACTAR analysis are based upon the conditions predicted by FIREBIRD in the slave channel analysis. In the case of the channel flow, since FACTAR is incapable of modelling flow reversal, the absolute value of the channel flow is used (*i.e.* flow is modelled as being always in the forward direction). The enthalpy used is also affected by FACTAR's inability to model coolant flow reversal. For the first two seconds, when the flow in the channel may be travelling simultaneously out of both ends of the channel, FACTAR applies the input coolant enthalpy transient to all axial locations. Hence, the enthalpy from the middle of the channel is used in the FACTAR input file for the first two seconds. For times after two seconds, the enthalpy of the incoming coolant is used. The relative power, channel flow, incoming coolant enthalpy, and channel pressure transients used in the FACTAR analysis are shown in Figures 2, 3, 4 & 5.

COMPRESS Input Data

COMPRESS version 1.0 (Reference (1)) was used to determine the free axial thermal expansion of each ring in the fuel string relative to the pressure tube and to determine the axial load transient required to accommodate any expansion in excess of the initial axial gap. COMPRESS credits elastic deformation of the fuel elements and of the pressure tube and plastic deformation of the bundle junctions, which are composed of the endcaps and endplates. Determination of the plastic deformation of the bundle junctions requires the temperature distribution in the junction components, which, as it is coupled to the deformation behaviour of the junction components, is determined with the COMPRESS code from the input data and the transient deformation.

COMPRESS 1.0 was developed and tested for New Brunswick Power as a prelude to this analysis. The code QA and validation included an independent line-by-line source code review and each subroutine was verified.

All of the required input data were extracted directly from the FACTAR output file, with the exception of the axial gap. The initial axial gap used for almost all cases is 25.4 mm (*i.e.* 1", slightly less than the minimum "as built" axial gap in the core under NOC shown in Table 1), with the exception of a series of sensitivity studies in which the initial axial gap was varied from 22.8 mm to 33.0 mm (*i.e.* 0.9" - 1.3"). The purpose of these cases was to determine the smallest initial axial gap for which no adverse results are predicted with respect to pressure tube integrity.

In order to assess the impact of certain assumptions which are internal to the COMPRESS code, some other sensitivity studies were undertaken through COMPRESS' input parameters. Specifically, the dimensions of the endcaps and endplates as modelled within COMPRESS were varied by 10%.

Another assumption in COMPRESS is that the temperature which controls the fuel thermal expansion is the temperature at the fuel land. The fuel land is the flat region of the pellet top just before the chamfer at the edge of the pellet. In reality, due to the cracked nature of the fuel element at power, the fuel land region would not be able to drive the axial thermal expansion of the fuel, but would redistribute its expansion in the crack volume. It is more likely that the axial thermal expansion of the fuel element would be controlled by the fuel average temperature. Therefore, the reference case was re-examined with the more realistic assumption that the fuel average temperature controls thermal expansion.

By default, COMPRESS allows contact conductance for the heat transfer between the fuel element and the main body of the endcap to be credited when the endcap projection reaches 25% strain. To test the sensitivity of the load predictions to this assumption, a case was performed in which the contact heat transfer between the fuel element and the endcap body is not credited at any time. Note that, since contact between the fuel element and the main body of the endcap is observed for high power fuel under normal operating conditions, this sensitivity is assessing additional conservatism, not reduced conservatism.

RESULTS

Channels B10, L11 and O06 with Both FIREBIRD and Maximum Initial Powers

The primary six cases analysed were the three channels for which FIREBIRD slave channel analysis was performed (B10, L11 and O06) at two different initial powers with a 25.4 mm initial axial gap. The two initial powers used were the power used in the FIREBIRD slave channel runs and the maximum possible power for the channel. Any sensitivity studies presented later in this paper are based on the most severe of the six cases presented in this section.

As an example, the FACTAR results for the case representing channel O06 using the FIREBIRD initial channel power and axial power profile is shown in some detail. The channel fuel average temperature transient is shown in Figure 6 to illustrate the timing of channel heatup and cooldown. The axial distribution of average temperatures is shown in Figure 7. The unconstrained thermal expansion of each fuel ring and of the pressure tube is shown for this channel in Figure 8.

For the present PLGS minimum axial gap of 67.81 mm, no fuel string compression is predicted for any of these cases. For the "as-built" minimum axial clearance of 25.55 mm, channel B10 has no axial contact at any initial power. Channel L11 shows axial compression of only 0.5 mm for the FIREBIRD initial channel power case. The other three cases result in axial contact and required deformation of channel components of 5 to 10 mm. Channel O06 with FIREBIRD initial channel power and axial power profile is the most severe in terms of the extent of fuel axial thermal expansion relative to the pressure tube and of the rate of thermal expansion after contact is predicted. Hence, this case results in the most severe peak load.

Figure 9 shows the axial load transient for the worst case, channel O06 with the FIREBIRD initial channel power and axial power profile, assuming an initial axial gap of 25.4 mm. The peak axial load is 23.85 kN. Therefore, the fuel elements would not bend into contact with the pressure tube for this case. Table 6 shows the peak temperatures achieved for this case by the endplate, the main body of the endcap and the endcap projections. The temperatures of the endcap and the endcap projections are high enough to allow plastic deformation, but are far from the melting temperature of Zircaloy. This shows that melting of bundle junction material, which could lead to pressure tube failure due to a localised hot spot on the pressure tube, does not occur.

Sensitivity to Fuelling Scenario

In order to assess the impact of the assumed average exit burnup used in determining the dwell times for the power/burnup histories in the factar_ss runs, the O06 case with the FIREBIRD initial powers was re-analysed for average exit burnups ranging in value from 10 MW·h/kgU to 340 MW·h/kgU.

The peak axial thermal expansion achieved in each scenario is summarised in Figure 10. The power/burnup history has a small effect on the peak fuel axial thermal expansion. The maximum fuel axial thermal expansion is for the nominal average exit burnup of 182 MW·h/kgU. No load assessments were carried out for these cases, as they are not significantly different from the case with a nominal fuelling scenario.

Sensitivity to COMPRESS Parameters

A series of sensitivity cases to COMPRESS input parameters has been performed on the channel O06 case with the *FIREBIRD initial* powers. These cases include a determination of the smallest initial axial gap for which fuel element buckling can be precluded.

The first set of sensitivity studies were to assess the impact of various assumptions made in the COMPRESS code. The assumptions examined pertain to the dimensions of the endcaps and endplates, the fuel temperature used as the basis of the fuel axial thermal expansion calculation and the heat transfer conditions between the fuel element and the endcap. The results of these cases are summarised in Table 7.

In COMPRESS, it is assumed that the heat flux from the fuel element into the endcap travels through three paths: firstly, the endcap projections are in physical contact with the element under NOC conditions, so there is a contact conductance (30 $kW/m^2 \cdot K$) through this interface and the heat travels through the projection, into the main endcap body and into the endplate and the coolant. Secondly, there is radiative heat transfer from the fuel element to the main body of the endcap. Lastly, once the endcap projections have strained by 25%, it is assumed that the main body of the endcap comes into contact with the fuel element directly. The resulting contact conductance is modelled to be 30 $kW/m^2 \cdot K$. To assess the impact of this bounding assumption, the O06 case with FIREBIRD initial powers was re-assessed with this last heat transfer mechanism disabled. The result can be seen in Table 7: the peak load is almost doubled without this axial contact heat transfer term. The results of examination of fuel bundles which have been irradiated show that there is actually contact between the fuel element and the main body of the endcap during normal operation in high power bundles, which are the bundles which experience the most significant compression. Therefore the results of this sensitivity study indicate that the estimate of axial load would be significantly lower if this contact were credited from time zero, instead of being credited only when the endcap projections have achieved a strain of 25%.

These sensitivity studies show that the assumptions made within COMPRESS are all either conservative with regard to the resulting peak axial load or are not parameters to which the analytical results are very sensitive.

The last input parameter whose sensitivity was examined in this analysis was the assumed value of the initial gap. In these sensitivity cases, the assumed axial gap is varied to determine the minimum axial gap for which there is no prediction of fuel element buckling. The assumed initial axial gap in the channel O06 case with FIREBIRD initial powers was 25.4 mm. Sensitivity studies were carried out in which this gap was set to 22.8 mm, 29.2 mm and 33.0 mm. The peak load predicted by COMPRESS for these cases and for the 25.4 mm gap case are summarised in Table 8. This table indicates that, if the axial gaps at PLGS are 25.4 mm (1.00") or greater, fuel element buckling could not occur for a 100% PSH Break and hence there would be no fuel channel integrity concern.

CONCLUSIONS

The results described in this paper show that, as long as the initial axial gap in any channel at PLGS is above 25.4 mm (1"), there is no threat to channel integrity due to fuel string compression during a 100% PSH Break, for a core at nominal equilibrium with 2 shutoff rods unavailable and a 2.3 mk void reactivity uncertainty. Since the 100% PSH break is the most severe recently-assessed LOCA scenario and since the limiting Large Break LOCA scenario bounds all other design basis accidents, it can be stated with confidence that this minimum acceptable axial gap applies to all design basis accidents.

The minimum axial gap in PLGS at 3880 FPD (May 1994) is 67.81 mm, more than twice the minimum acceptable axial gap. If PLGS is retubed, the minimum axial gap in any channel should not be allowed to be less than 25.4 mm without a detailed assessment of the effect on pressure tube integrity of a fuel element bending into contact with the pressure tube.

REFERENCES

(1) P.J. Reid, "COMPRESS - A Code to Determine Axial Loads due to Fuel String Compression due to Axial Thermal Expansion", PLGS IR-0553-05, July 1994

(2) H.E. Sills & Y. Liu, "FACTAR_SS 1.0: A Computer Program to Model Fuel Behaviour Under Normal Operating Conditions for a Single Channel in a Reactor Core", OH RSOAD N-03553-940033, March 22 1994

(3) H.E. Sills, S.L. Wadsworth, L.J. Watt & P.J. Reid, "FACTAR 1.0, Fuel And Channel Temperature And Response: Part 1, Model Description and User Manual", OH RSOAD N-03353-940031, January 18 1994

(4) R.E. Williford, "A Cracked Fuel Constitutive Equation", Vol. 67, Nuclear Technology, November 1984

(5) "ASTM Standard Specification for Hot-Rolled and Cold-Finished Age Hardening Stainless and Heat-Resisting Steel Bars, Wire, And Shapes", ASTM A 564-84, September 1984

TABLE 1: MINIMUM "AS-BUILT" AXIAL GAPS AT FULL POWER (mm)

Most limiting channel

	1	2	3	4	5	6	7	8	9	10	11	12	13	14	15	16	17	18	19	20	21	22	
A									57.45	56.79	[illegible]	55.83	57.10	56.01									A
B						57.91	56.36	56.62	41.33	42.04	[illegible]	44.88	40.34	40.79	55.85	55.78	55.55						B
C					56.97	40.89	41.45	40.36	25.86	26.24	26.54	28.02	27.81	26.59	42.37	42.24	42.82	56.87					C
D				58.12	42.47	29.16	27.08	28.17	28.02	29.92	29.11	28.55	27.46	27.94	28.09	29.18	27.46	42.77	57.99				D
E			58.14	42.37	27.56	27.84	28.17	27.71	28.30	27.46	27.53	28.09	27.71	28.09	27.20	26.52	27.46	27.66	42.70	57.73			E
F			58.62	43.15	27.69	29.13	27.51	27.94	28.17	28.07	27.79	27.91	27.71	28.35	27.66	28.73	28.35	[illegible]	42.67	58.57			F
G		57.81	42.77	27.81	27.97	27.66	26.92	26.80	26.52	26.75	27.08	27.76	27.03	27.23	26.64	26.44	26.11	26.82	26.57	41.10	57.51		G
H		57.56	41.99	27.66	27.36	26.67	27.18	27.56	25.81	26.95	28.30	26.39	27.10	26.57	28.19	27.33	27.46	26.82	27.97	42.65	59.08		H
J	58.09	42.34	27.64	26.31	27.58	27.30	27.10	28.65	28.32	27.91	27.86	28.09	27.69	27.99	27.94	26.34	28.27	27.56	27.71	27.46	43.08	57.89	J
K	58.34	43.84	27.64	28.17	62.26	28.02	27.43	27.71	27.91	27.46	27.23	27.43	27.94	27.58	26.59	27.30	26.90	27.66	27.20	28.91	41.66	57.05	K
L	57.86	42.57	27.84	27.61	27.38	27.56	28.47	28.80	29.24	26.95	27.18	27.56	27.38	27.56	28.47	28.14	28.04	26.97	27.76	28.19	42.60	57.28	L
M	58.70	44.17	27.84	28.80	27.08	28.83	28.40	28.91	27.86	27.46	27.86	27.86	27.33	27.84	27.36	27.81	27.51	27.84	27.15	27.20	42.65	57.10	M
N	57.58	43.15	27.58	27.53	26.77	26.82	27.51	26.90	27.18	27.84	28.60	28.63	27.43	26.87	27.20	26.95	25.76	26.95	26.57	26.52	42.04	57.35	N
O	59.59	42.72	27.61	28.12	26.95	27.41	27.46	27.38	27.15	26.82	28.47	26.34	27.28	27.69	27.86	27.05	27.46	27.33	27.03	27.33	42.34	57.79	O
P		57.23	41.48	27.64	27.71	27.58	26.44	27.56	26.85	27.61	**25.55**	26.11	27.03	27.74	26.87	27.05	26.72	27.20	26.39	42.21	56.72		P
Q		57.00	41.53	25.78	27.23	26.77	27.00	26.87	26.72	26.14	26.19	26.14	26.77	26.87	27.08	26.39	25.58	26.24	27.05	41.38	57.58		Q
R			56.01	40.64	26.72	26.09	26.57	26.42	25.78	25.98	26.70	26.70	27.05	25.83	26.44	25.73	25.78	26.47	40.79	55.52			R
S			57.28	41.61	26.42	26.21	26.64	27.36	27.36	27.71	26.62	26.77	26.67	26.82	25.98	26.95	26.72	27.28	41.63	58.62			S
T				57.02	43.31	28.63	27.99	26.47	27.79	27.13	27.08	26.82	27.48	27.13	27.33	27.30	26.80	42.49	57.76				T
U					57.94	43.61	43.10	42.95	27.61	27.89	26.97	27.10	26.52	27.56	43.10	41.73	42.49	58.27					U
V						56.44	58.22	56.95	42.75	42.62	43.36	41.88	42.16	42.21	57.63	58.42	57.99						V
W									58.29	57.84	57.30	58.50	58.55	[illegible]									W
	1	2	3	4	5	6	7	8	9	10	11	12	13	14	15	16	17	18	19	20	21	22	

TABLE 2:MINIMUM AXIAL GAPS AT 3880 FPD (MAY 1994) AT FULL POWER (mm)

Most limiting channel

	1	2	3	4	5	6	7	8	9	10	11	12	13	14	15	16	17	18	19	20	21	22	
A									86.64	86.78	90.57	86.09	83.69	84.09									A
B						75.69	87.31	93.77	79.82	85.39	85.24	89.91	86.76	81.19	92.90	87.76	84.57						B
C					85.17	78.79	82.78	87.07	[illegible]	85.43	79.46	79.29	80.67	80.72	95.38	86.62	79.46	87.98					C
D				83.52	82.51	68.15	77.68	84.73	90.88	85.49	87.14	80.27	96.20	93.01	89.39	87.18	75.71	84.04	87.99				D
E			85.57	83.01	77.85	86.48	79.65	94.56	84.69	92.02	91.27	92.53	81.13	82.10	96.08	90.10	83.43	80.52	82.41	86.38			E
F			93.30	88.34	85.68	80.74	94.91	96.84	81.35	94.72	91.54	94.02	102.4	91.96	99.70	92.35	87.14	79.92	92.89	95.23			F
G		85.08	84.82	77.40	93.03	91.88	91.27	88.10	88.48	89.98	89.02	94.44	102.3	91.82	92.87	91.05	82.90	86.59	81.31	84.24	90.55		G
H		96.02	91.59	83.51	88.44	90.82	93.09	83.49	98.44	98.51	101.1	98.44	93.69	97.41	101.3	91.72	94.32	81.71	79.16	91.77	97.44		H
J	87.94	85.00	77.06	74.69	82.59	87.61	86.48	92.81	99.17	86.56	91.81	93.59	86.62	93.21	97.31	95.36	92.84	94.30	86.21	82.11	87.06	87.87	J
K	89.22	86.59	72.49	94.85	85.77	91.87	99.91	97.43	94.45	89.96	98.04	93.80	82.77	83.09	84.05	95.92	94.03	88.42	92.84	74.53	88.61	91.58	K
L	94.48	87.02	84.09	90.62	99.13	94.40	95.81	94.92	94.80	89.32	88.09	96.59	87.60	95.30	94.83	86.17	87.83	89.93	87.68	77.65	91.56	91.52	L
M	94.23	90.60	74.33	93.66	97.30	96.68	90.97	93.07	93.16	89.71	96.22	90.75	92.82	95.94	98.91	90.71	87.50	96.83	88.91	84.53	91.00	91.34	M
N	88.71	87.11	87.55	93.81	92.39	92.67	92.05	96.38	91.26	94.38	92.57	96.01	91.97	87.31	82.70	87.54	91.54	90.18	93.04	85.57	85.98	88.60	N
O	89.28	86.30	85.82	88.95	83.96	103.1	93.09	94.90	97.85	84.36	97.34	87.29	88.95	97.01	93.43	93.09	99.04	89.25	87.83	73.89	86.03	83.99	O
P		91.84	93.10	81.47	92.34	80.18	94.08	100.6	89.91	81.32	93.37	93.85	94.69	95.38	97.00	86.82	93.69	86.94	86.77	90.09	93.56		P
Q		82.50	86.80	73.75	76.60	90.04	78.98	96.67	87.01	89.25	87.57	93.44	80.15	90.76	80.01	83.12	83.66	82.22	73.07	84.00	88.10		Q
R			88.21	88.84	74.33	75.66	92.07	87.66	91.98	92.61	90.55	94.26	87.77	88.22	91.52	76.24	86.35	82.89	88.91	94.14			R
S			84.70	80.21	75.10	74.90	81.06	88.06	81.15	93.49	93.18	88.92	89.33	91.69	89.68	78.22	77.49	78.99	80.96	82.59			S
T				82.33	80.09	70.06	77.51	77.10	82.52	90.44	83.30	89.21	92.67	81.38	84.74	80.17	70.87	78.82	91.06				T
U					86.25	76.91	83.97	88.09	79.06	79.56	76.48	78.14	74.47	74.43	89.69	83.98	76.41	84.83					U
V						74.31	95.00	97.50	79.75	84.33	83.68	80.64	80.97	75.58	81.75	81.23							V
W									82.75	81.91	81.78	81.56	85.04	85.85									W
	1	2	3	4	5	6	7	8	9	10	11	12	13	14	15	16	17	18	19	20	21	22	

TABLE 3: ASSUMED VALUES OF VARIOUS PARAMETERS FOR FACTAR_SS, FACTAR AND COMPRESS (* DENOTES A PARAMETER WHOSE IMPACT IS ASSESSED IN A SENSITIVITY STUDY

Parameter	Value	Reference/Justification
Relative Element Power	See Table 5	Design values
Nominal Average Exit Burnup*	182 MW·h/kgU	Representative of nominal fuelling
Axial Power Profile*	See Table 4	Consistent with FIREBIRD Analysis
Power/Burnup Envelope	see Figure 1	License limit
Bundle Shift Scheme	8 bundle shift	Representative of nominal fuelling
Fuel Geometry	Nominal Design	Representative of actual fuel
Fuel Stack Length	Nominal Design	For factar_ss analysis
Fuel Stack Length	Nominal Design + 0.4%	For FACTAR and COMPRESS only
Density	10.6 Mg/m^3	Representative of normal fuel
Young's Modulus of Sheath	79.2 GPa	Value for Zircaloy-4
Sheath thermal expansion coeff.	6.5 10^{-6} K^{-1}	Value for Zircaloy-4
Film HTC for NOC	50.0 $kW/m^2 \cdot K$	Nominal values
Coolant Temperature for NOC	562 K	Nominal value
Coolant Pressure for NOC	10.555 MPa	Consistency with FIREBIRD data
Channel Dimensions	Nominal Design	Representative uncrept values
Radiative Heat Transfer Model	On	Required for appropriate modelling
Coolant Mixing Option	Partial Mixing	Maximises fuel temperatures
Pressure Tube Strain Calculation	On	Required for appropriate modelling
Thermal Hydraulic Time Step	0.2s for t<25s	Required for appropriate modelling
Oxidation Model	FROM	Required for appropriate modelling
Thermal Hydraulic Transients	See Figures 3, 4 & 5	Derived from FIREBIRD Analysis
Normalised Power Transient	See Figure 2	Consistent with FIREBIRD Analysis
Initial Axial Gap*	32.9 mm	Minimum "as-built" gap

TABLE 4: AXIAL POWER PROFILES USED IN FACTAR ANALYSIS

Bundle	B10, FIREBIRD Powers	B10, Maximum Powers	L11, FIREBIRD Powers	O06 & L11, Max. Powers	O06, FIREBIRD Powers
1	92.6	114.8	171.8	155.5	166.6
2	233.3	298.0	387.3	387.6	401.5
3	363.6	479.8	521.5	572.3	586.1
4	464.5	641.6	568.9	705.3	722.4
5	539.0	756.9	651.6	856.3	841.0
6	569.2	806.5	689.0	927.1	885.5
7	566.7	804.3	686.0	935.1	882.9
8	532.6	751.5	642.5	866.5	834.0
9	465.9	636.9	578.7	705.2	740.0
10	371.0	485.0	558.4	598.6	624.1
11	240.5	305.9	428.7	418.3	435.9
12	94.8	118.6	189.1	171.6	179.9
Total	4533.8	6199.9	6073.5	7300.0	7300.0

TABLE 5: RADIAL POWER DISTRIBUTION USED IN FACTAR ANALYSIS

Element Ring (Number of Elements)	Relative to Average	Relative to Outer	% Power per Element	% Power per Ring
Outer (18)	1.1310	1.000	3.057	55.03
Intermediate (12)	0.9206	0.814	2.488	29.86
Inner (6)	0.8051	0.712	2.176	13.06
Centre (1)	0.7613	0.673	2.058	2.058
			TOTAL:	100.0

TABLE 6: MAXIMUM BUNDLE JUNCTION TEMPERATURES FOR CHANNEL O06 "NOMINAL" CASE

Bundle Junction Component	Peak Temperature (°C)
Endplate	819.73
Endcap Body	1049.4
Endcap Projections	1081.3

TABLE 7: SENSITIVITY STUDIES ON COMPRESS INTERNAL ASSUMPTIONS

Case Description	Peak Axial Load (kN)
Reference Case	23.85
Reference Case, but Bundle Junction Load Bearing Areas Increased by 10%	24.84
Reference Case, but Bundle Junction Thicknesses Reduced by 10%	22.95
Reference Case, but Fuel Average Temperature used for Thermal Expansion	1.76
Reference Case, but Contact Heat Transfer to Main Endcap Body Disabled	41.48

TABLE 8: SENSITIVITY STUDIES ON INITIAL CHANNEL AXIAL GAP

Case Description	Peak Axial Load (kN)
Reference Case	23.85
Reference Case, but Initial Gap of 22.8 mm	36.89
Reference Case, but Initial Gap of 29.2 mm	14.37
Reference Case with Initial Gap of 33.0 mm	3.33

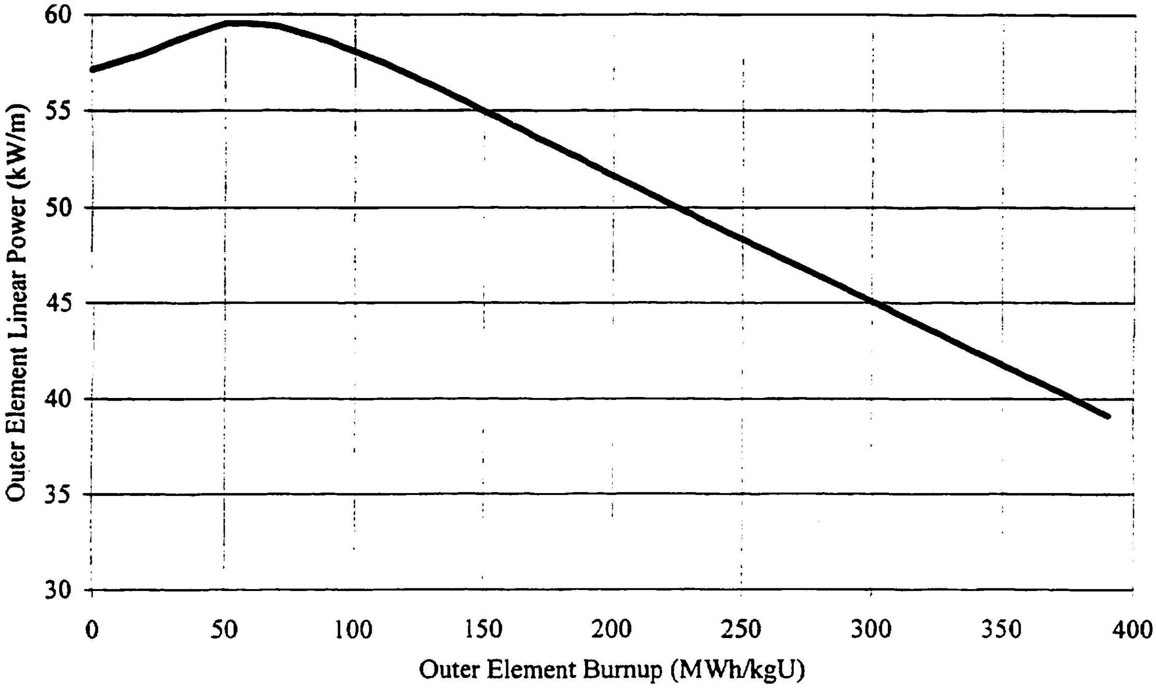

FIGURE 1: LICENSING OVERPOWER ENVELOPE

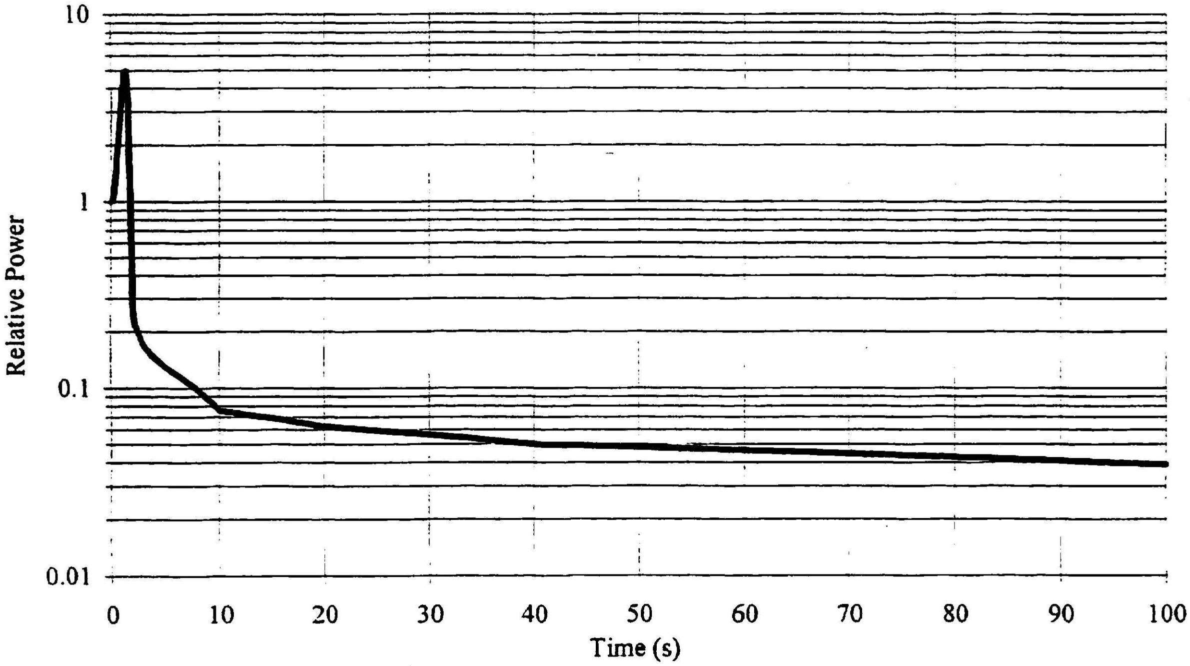

FIGURE 2: RELATIVE OVERPOWER TRANSIENT USED IN FACTAR ANALYSIS

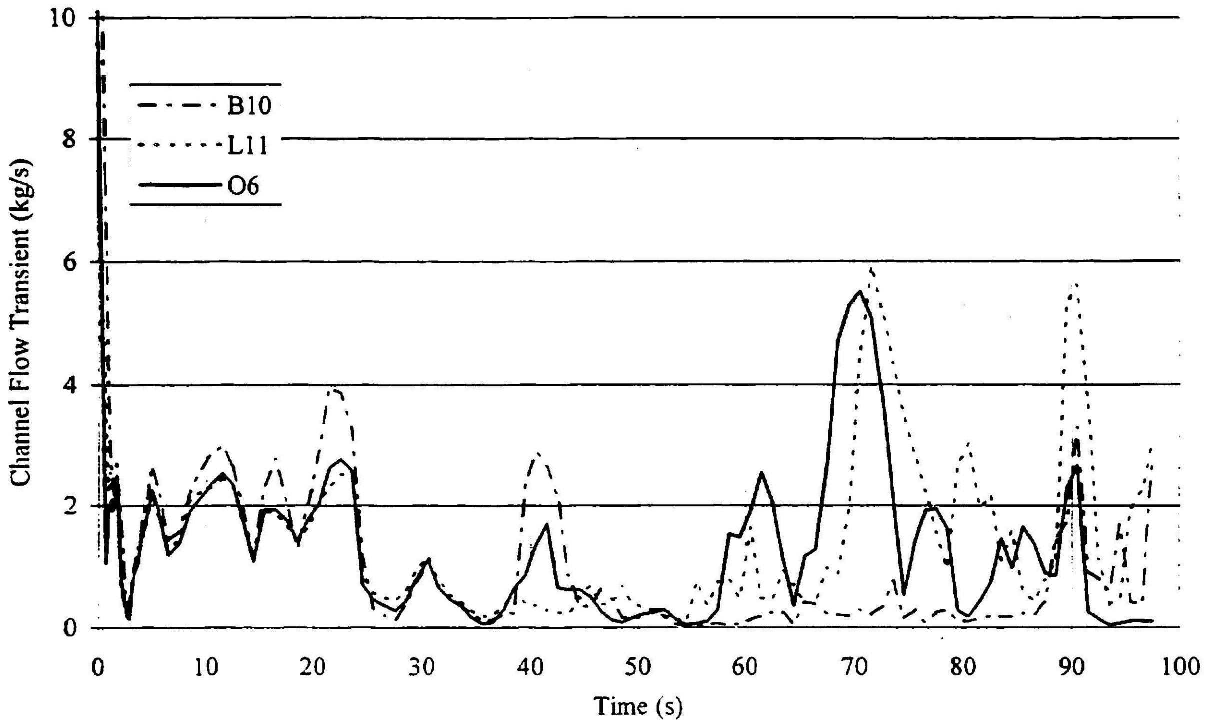

FIGURE 3: CHANNEL FLOW TRANSIENTS USED IN FACTAR ANALYSIS

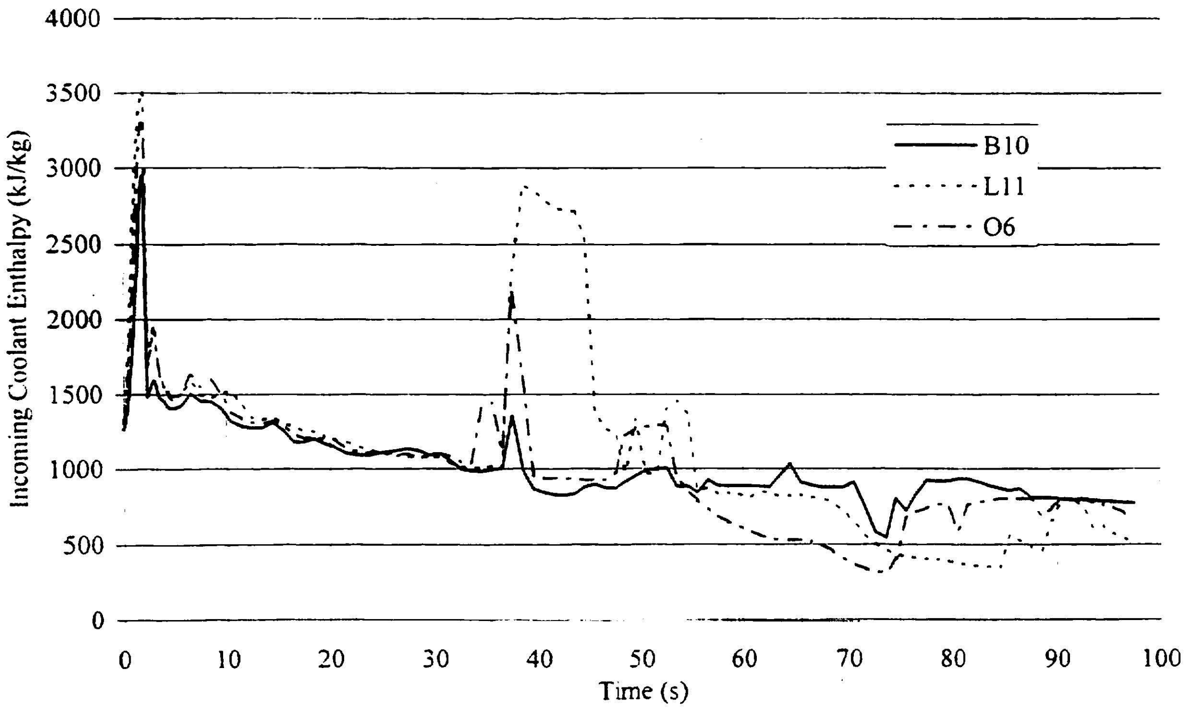

FIGURE 4: INCOMING COOLANT ENTHALPY TRANSIENTS USED IN FACTAR ANALYSIS

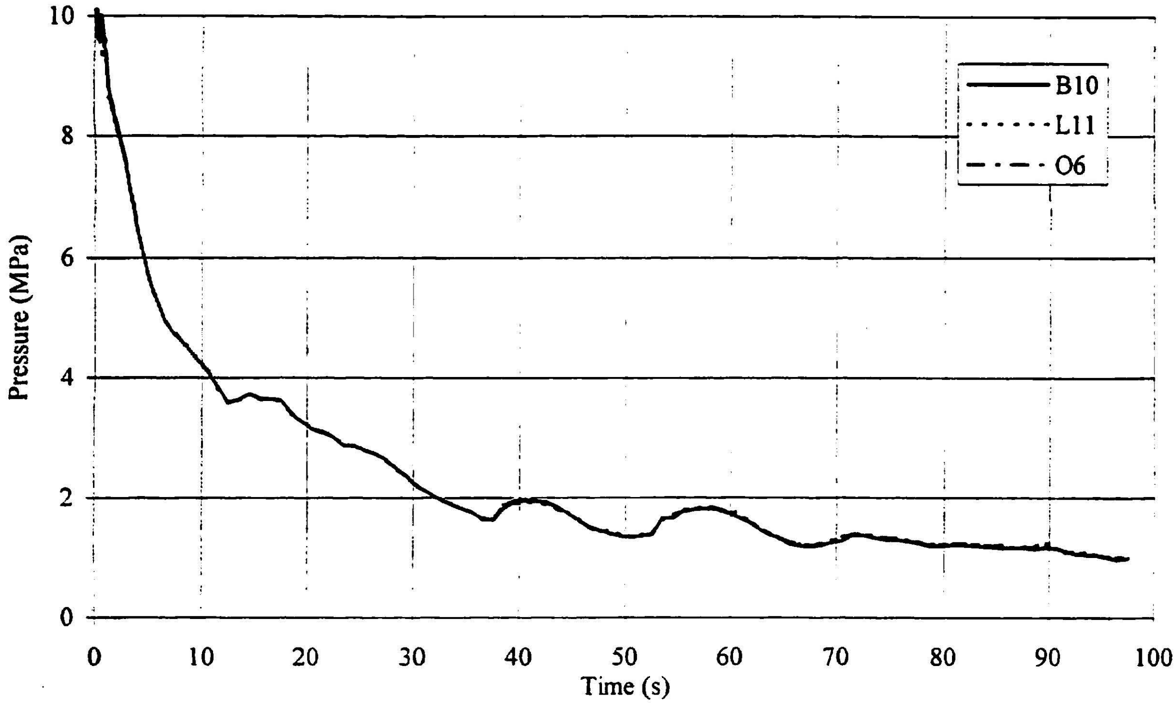

FIGURE 5: CHANNEL PRESSURE TRANSIENTS USED IN FACTAR ANALYSIS

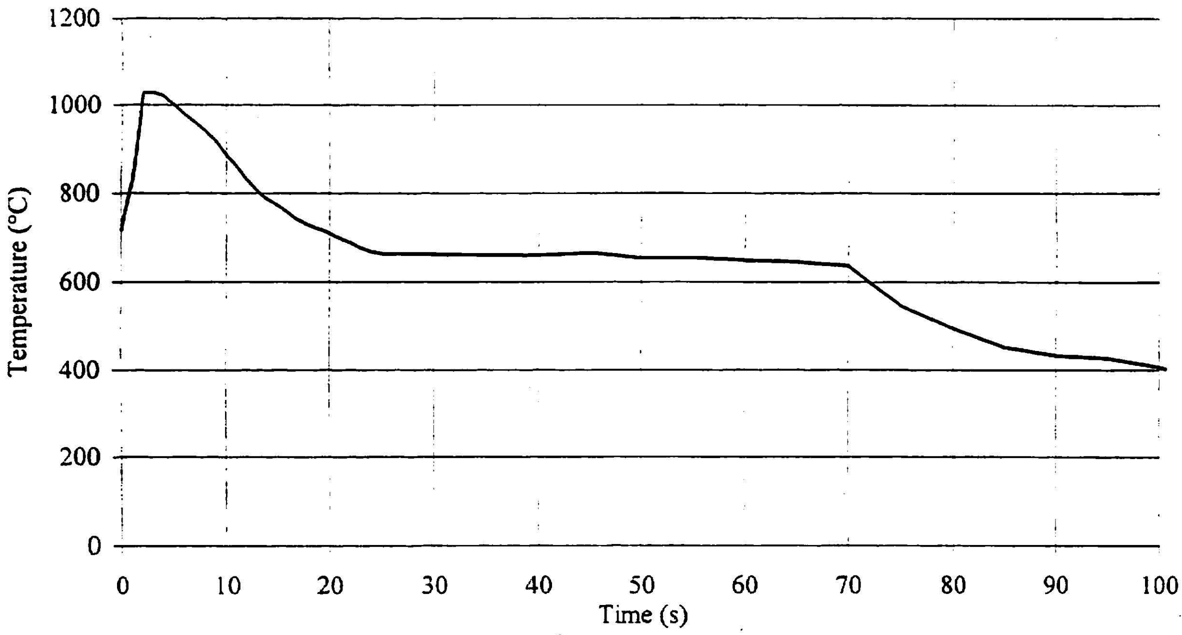

FIGURE 6: CHANNEL AVERAGE FUEL TEMPERATURE TRANSIENT FOR CHANNEL O06 WITH FIREBIRD INITIAL POWERS

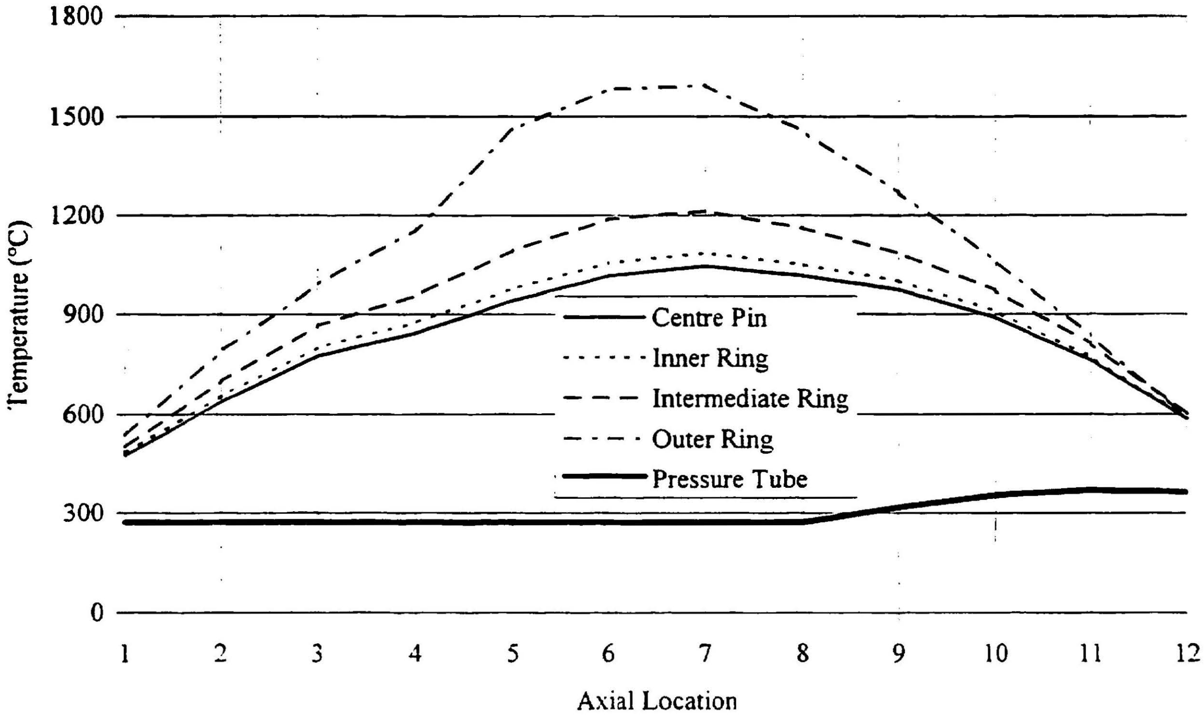

FIGURE 7: AVERAGE TEMPERATURE DISTRIBUTION AT 5 SECONDS FOR CHANNEL O06 WITH FIREBIRD INITIAL POWERS

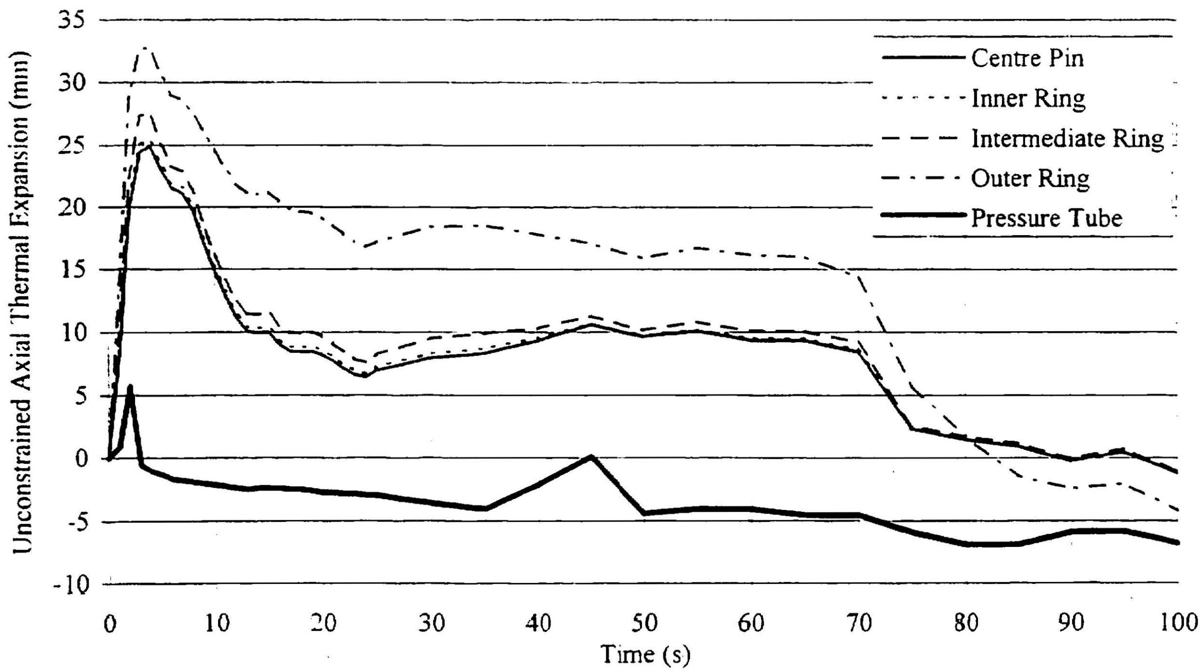

FIGURE 8: UNCONSTRAINED TRANSIENT AXIAL THERMAL EXPANSION FOR CHANNEL O06 WITH FIREBIRD INITIAL POWERS

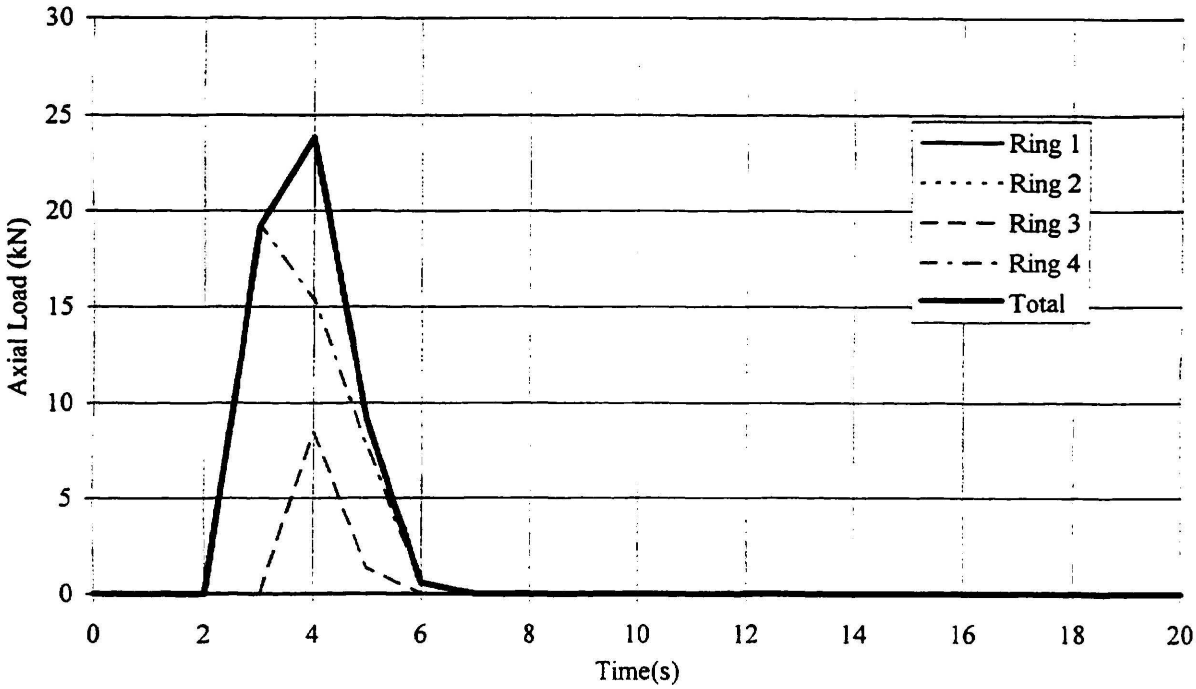

FIGURE 9: AXIAL LOAD TRANSIENT FOR CHANNEL O06 WITH FIREBIRD INITIAL POWERS

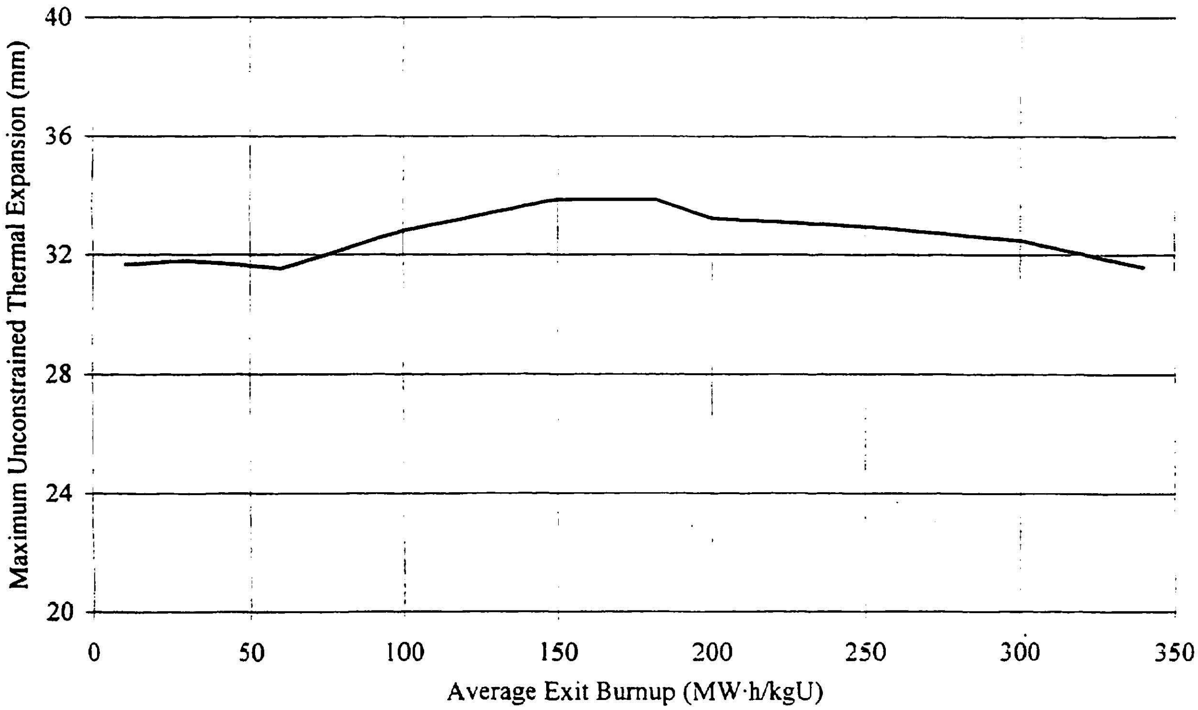

FIGURE 10: SENSITIVITY OF UNCONSTRAINED AXIAL EXPANSION OF CHANNEL O06 WITH FIREBIRD INITIAL POWERS TO AVERAGE EXIT BURNUP